Electronic Supplementary Material (ESI) for Journal of Materials Chemistry A.

Supporting Information (SI)

Aqueous "Polysulfide-ene" Polymerization for Sulfur-Rich Nanoparticles and Their Use in Heavy Metal Ion Remediation

Hyuksoo Shin,[a] Jihee Kim,[b] Dowan Kim,[a] Viet Huu Nguyen,[b] Sangwook Lee,[b] Seunghee Han,[b,] Jeewoo Lim,[c,]* and Kookheon Char[a,]**

[a]*School of Chemical and Biological Engineering, Seoul National University, Seoul 08826, Republic of Korea*

[b]*School of Earth Science and Environmental Engineering, Gwanju Institute of Science and Technology, Gwangju, 61005, Republic of Korea*

[c]*Department of Chemistry, Kyung Hee University, Seoul, 02447, Republic of Korea*

1 Supporting Tables

Table S1. Characterization of PS_nDVSs.

	PS_2DVS	PS_3DVS	PS_4DVS
Glass Transition Temperature (T_g) (°C)	11.6	8.6	13.7
Zeta Potential (mV)	32.2	34.8	32.9
Size (nm)	223	300	233
Size Polydispersity (σ^2/d^2)	0.028	0.022	0.056

Table S2. Elemetal analysis of PS_nDVSs.

	PS_2DVS		PS_3DVS		PS_4DVS	
	Theoretical Value (%)	Experimental Value (%)	Theoretical Value (%)	Experimental Value (%)	Theoretical Value (%)	Experimental Value (%)
Carbon	24.4	26.0	20.1	22.2	18.1	19.3
Hydrogen	3.9	4.4	3.3	3.7	2.8	3.3
Sulfur	56.1	52.2	62.2	59.3	65.9	64.5
Oxygen	15.6	17.4	14.6	14.8	13.2	12.9
Total	100	100	100	100	100	100

Table S3. Mercury ion sorption isotherm of PS_nDVS-SHs

Initial Conc. (ppm)	PS_2DVS-SH	PS_3DVS-SH	PS_4DVS-SH
	Equilibrium Conc. (ppm) (Standard Deviation)		
245	0.39 (0.34)	0.04 (0.52)	1.03 (0.64)
454	0.75 (-)	0.575 (0.05)	0.93 (0.59)
528	1.42 (13)	2.446 (102)	2.45 (5.20)
1011	209 (27.08)	295.95 (3.75)	277.55 (5.30)
2164	1333 (50.20)	1333.85 (8.70)	1319.3 (-)
2823	2059 (1.20)	2060 (0.7)	2060 (0.70)
4796	3863 (0.90)	4796 (-)	3841 (0.50)

Table S4. Mercury ion sorption performance of materials.

Adsorbend	K_d (mL g^{-1})	q_{max} (mg g^{-1})	Remaining Hg^{2+} Concentration
PS_2DVS-SH	2.2E7	9200	0.005 ppm
PAF-1-SH	5.76E7	1014	0.4 ppb
POP-SH	5.50E8	1216	<0.1 ppb
FMMS	3.40E5	505	0.7 ppb
Chalcogel-1	1.61E7	645	0.04 ppm
W-DR-N-MoS_2	3.53E8	2563	0.2 ppb
Zr-DMBD	9.99E5	179	<0.01 ppm
68(W)	6.90E6	2173	0.45 ppm
TAPB-BMTTPA-COF	7.82E5	734	0.01 ppm
TPB-DMTP-COF-SH	3.23E9	4395	1.5 ppb
COF-S-SH	2.30E9	1359	<0.1 ppb

Table S5. Ion selectivity tests for PS_nDVS-SH in mixed metal ion solution.

	Initial Conc. (ppb)	PS_2DVS-SH	PS_3DVS-SH	PS_4DVS-SH
		Equilibrium Conc. (ppb) (Removal Efficiency (%))		
Hg^{2+}	10770	11 (99.90)	9 (99.91)	4 (99.96)
Mg^{2+}	12190	9797 (19.63)	10074 (17.36)	10182 (16.48)
Zn^{2+}	14734	12733 (13.58)	11569 (21.48)	11664 (20.84)
Na^{+}	11024	11576 (-5.00)	9562 (13.26)	9745 (11.60)
K^{+}	11660	10450 (10.38)	10339 (11.33)	10207 (12.46)
Ca^{2+}	8809	7051(19.96)	7545 (14.34)	8108 (7.96)
Pb^{2+}	1224	475 (61.18)	266 (78.24)	17 (98.59)
Cd^{2+}	12296	5314 (56.78)	3389 (72.44)	34 (99.73)

2 **Supporting Figures**

Figure S1. ^{1}H NMR spectra of divinyl sulfone and polysulfide with sodium sulfonate standard in D_2O for kinetic study of PS_nDVS.

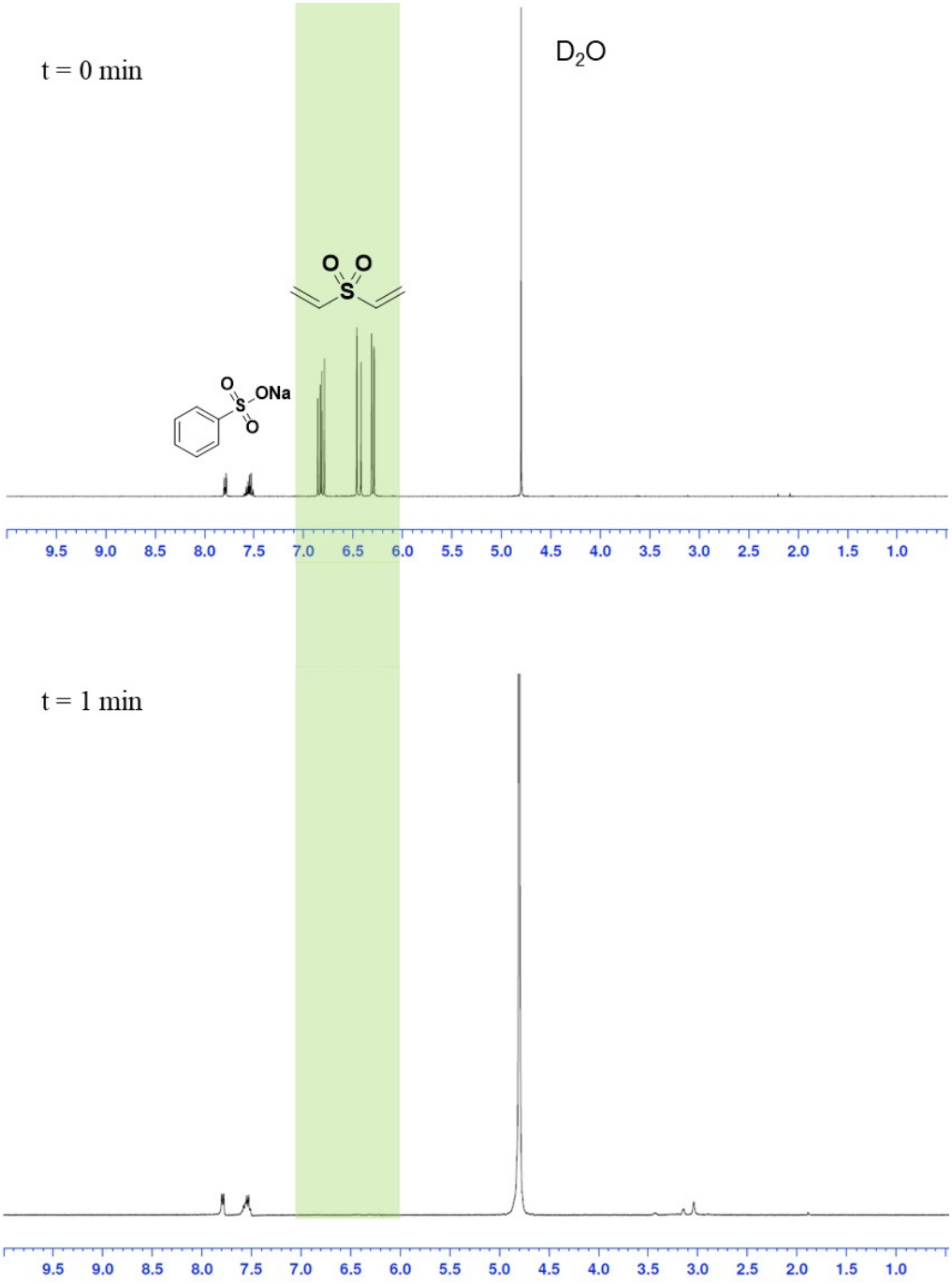

Figure S2. SEM images of PS_nDVS synthesized with and without various surfactants; (a) without surfactant; (b) Triton X-100; (c) polyvinylpyrrolidone; (d) sodium dodecyl sulfate. Scale bars in SEM images are 1 μm.

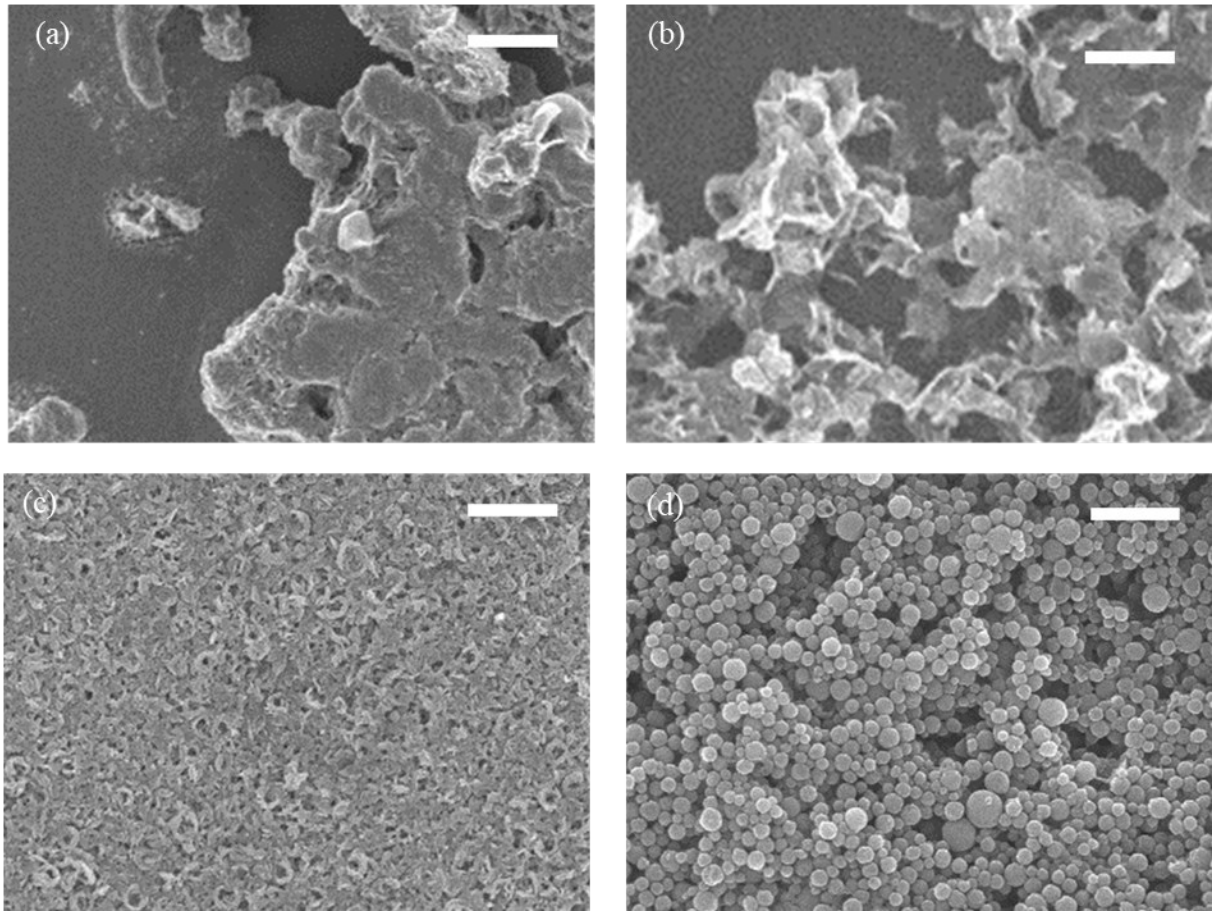

Figure S3. SEM image of PS_4DVS as synthesized (left), after dispersing in pH 3 solution for 24 hours (center), and after immersing in pH 12 solution for 24 hours (right).

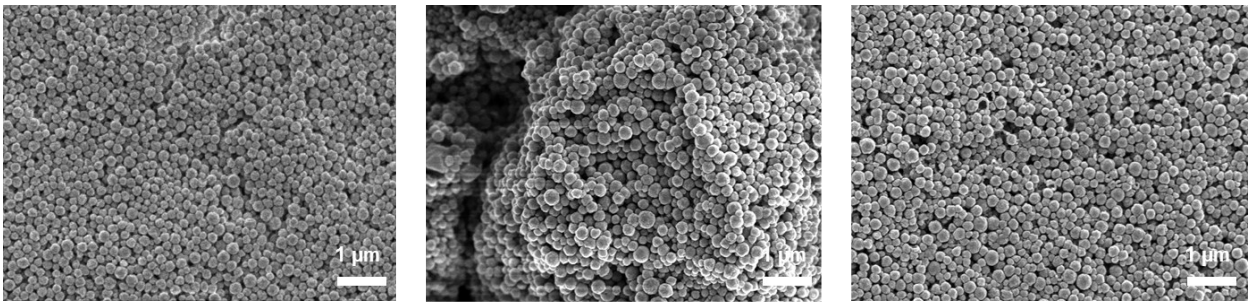

PS_4DVS **PS_4DVS pH3, 24 hr** **PS_4DVS pH12, 24 hr**

Figure S4. (a) Adsorption isotherm of PS_2DVS; (b) Langmuir isotherm of PS_2DVS.

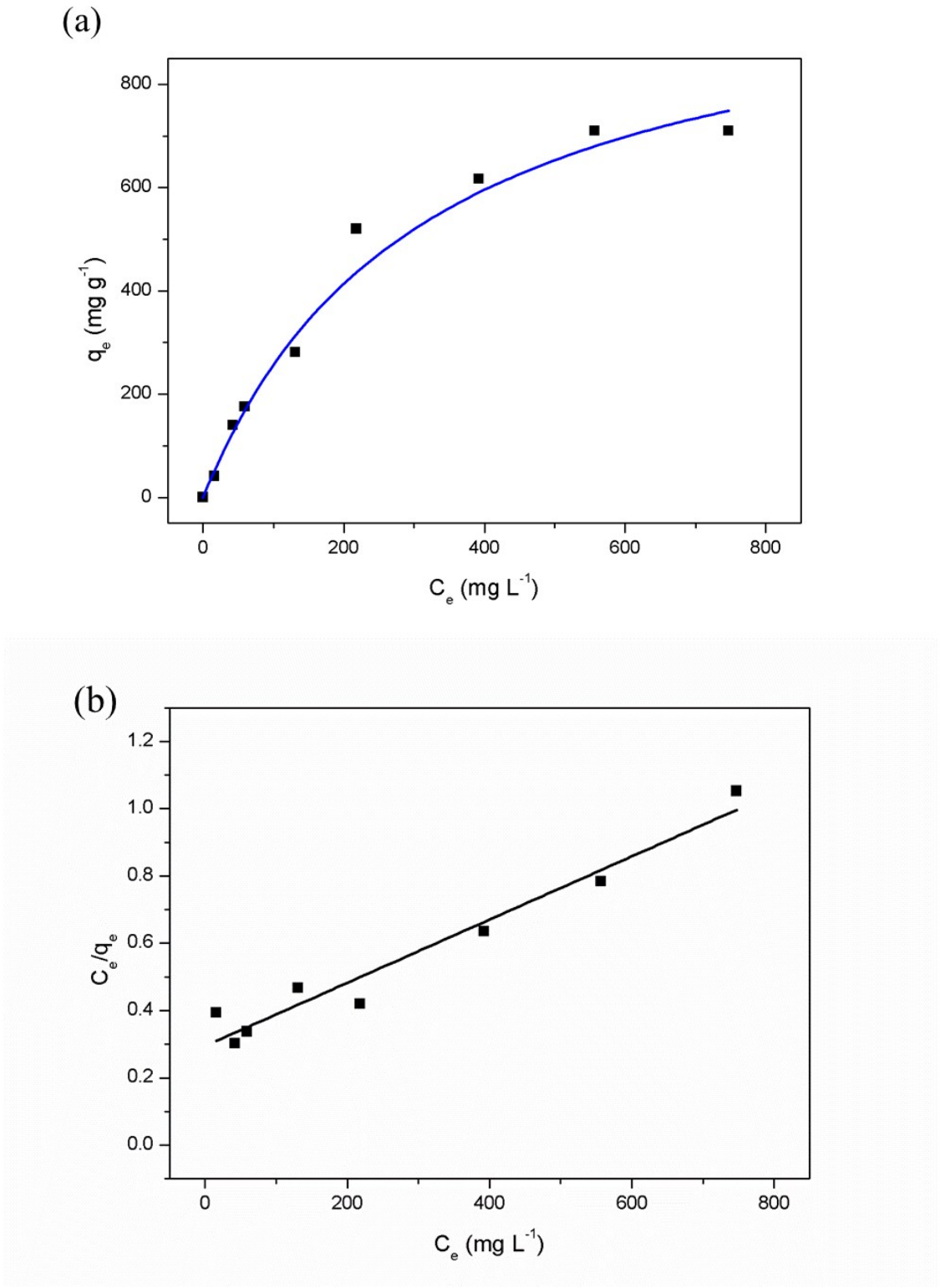

Figure S5. SEM image of PS_4DVS-SH nanoparticles.

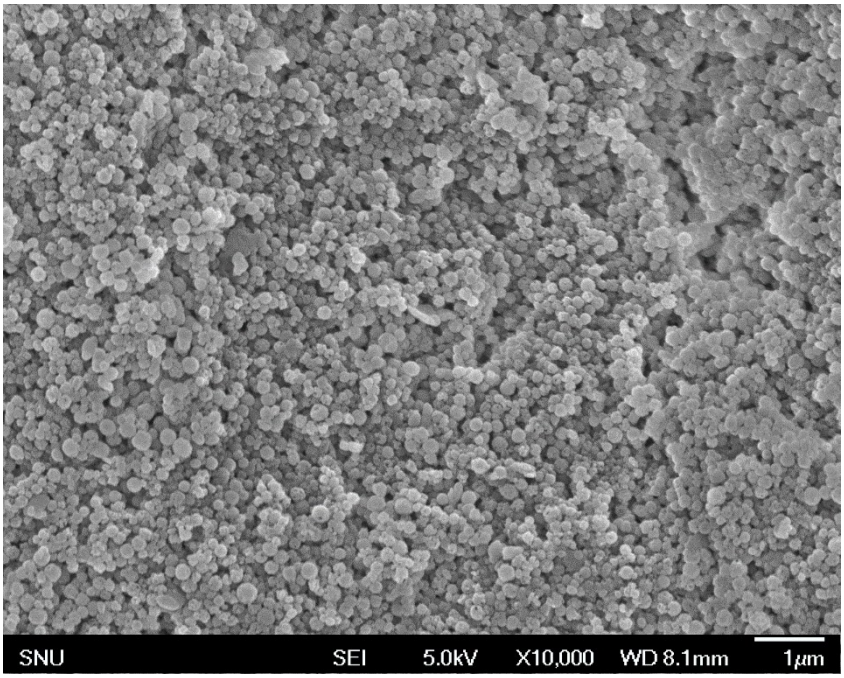

Figure S6. TGA of PS_4DVS and PS_4DVS-SH.

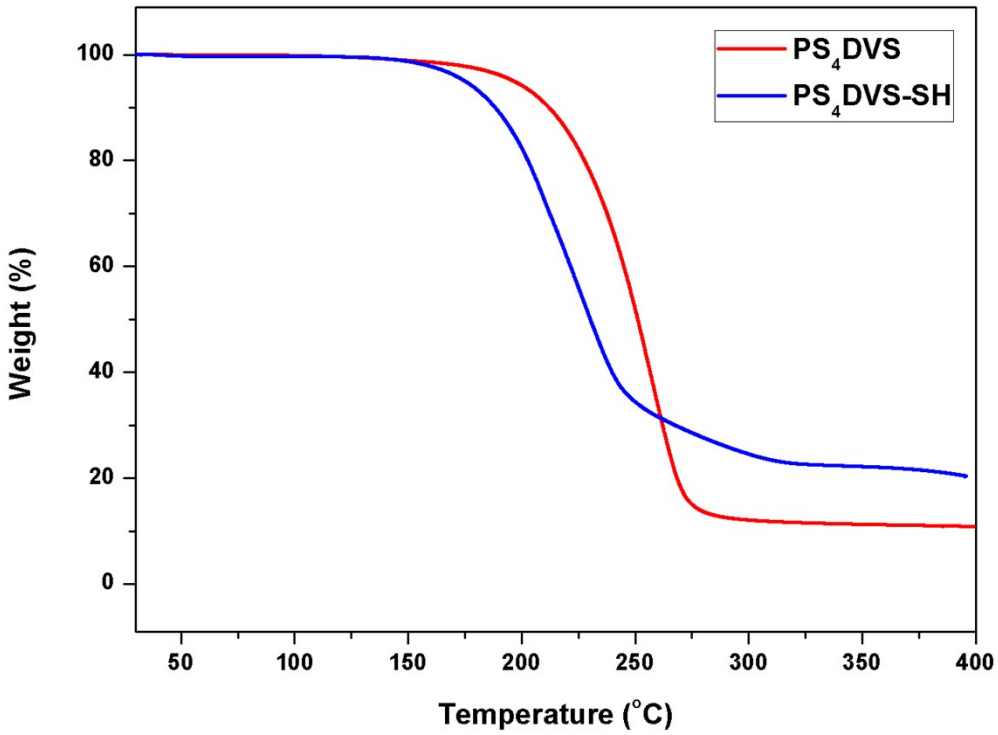

Figure S7. the Langmuir isotherm plots for the adsorption isotherms of PS_2DVS-SH, PS_3DVS-SH, and PS_4DVS-SH.

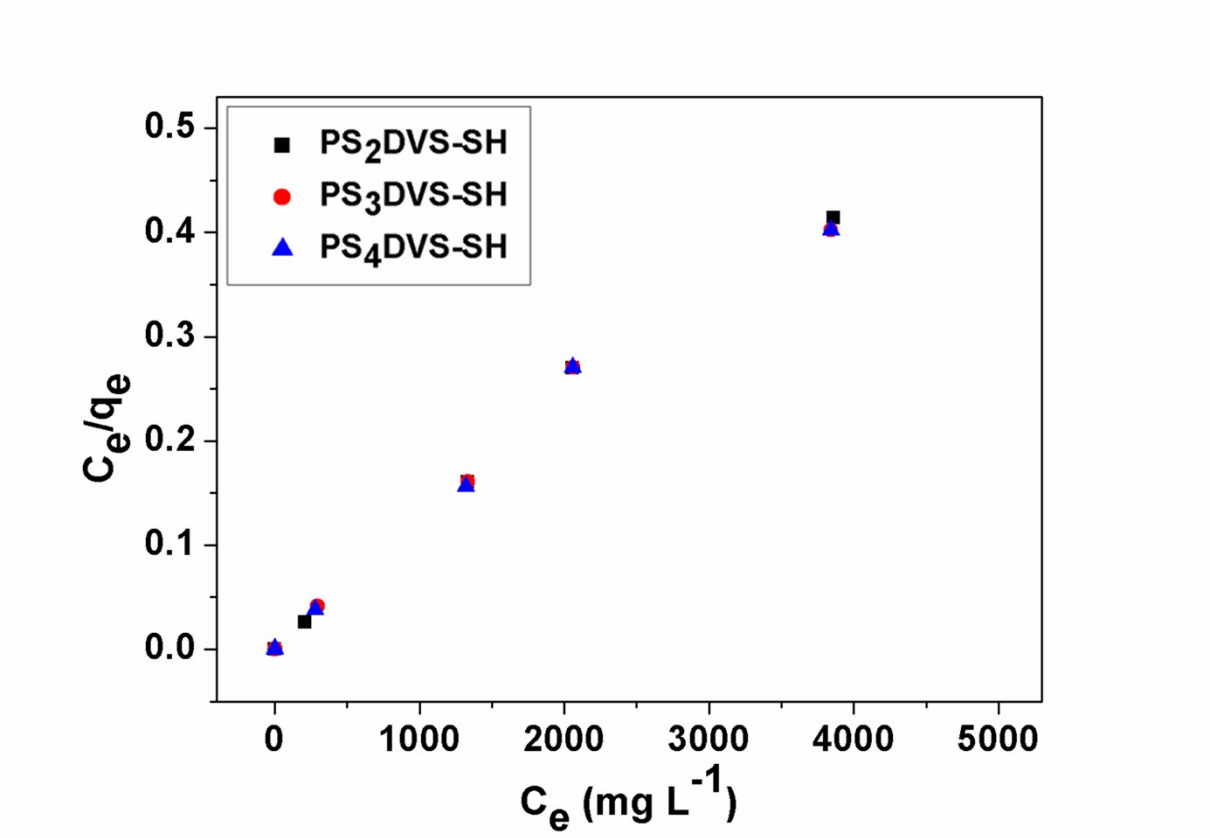

Figure S8. Mercury adhesion of PS4DVS-SH with and without TCEP at 5000 ppm Hg^{2+} solution. The adsorption was carried out for 24 hours at room temperature in acetate buffer at pH = 3.7.

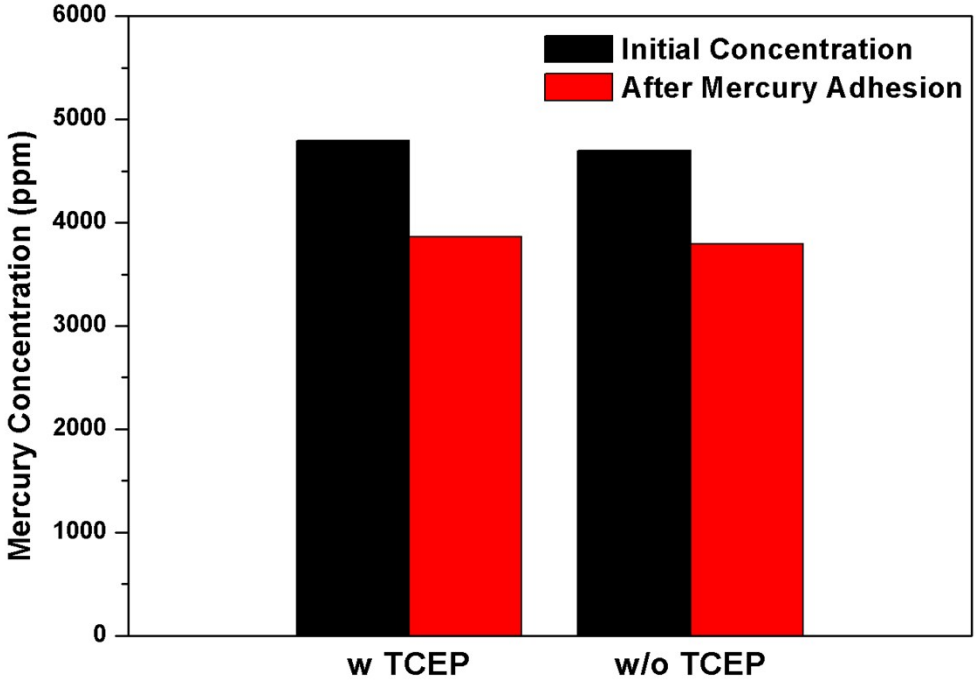

Figure S9. The kinetic investigation of PS_2DVS-SH fitted with the pseudo-second-order kinetic model.

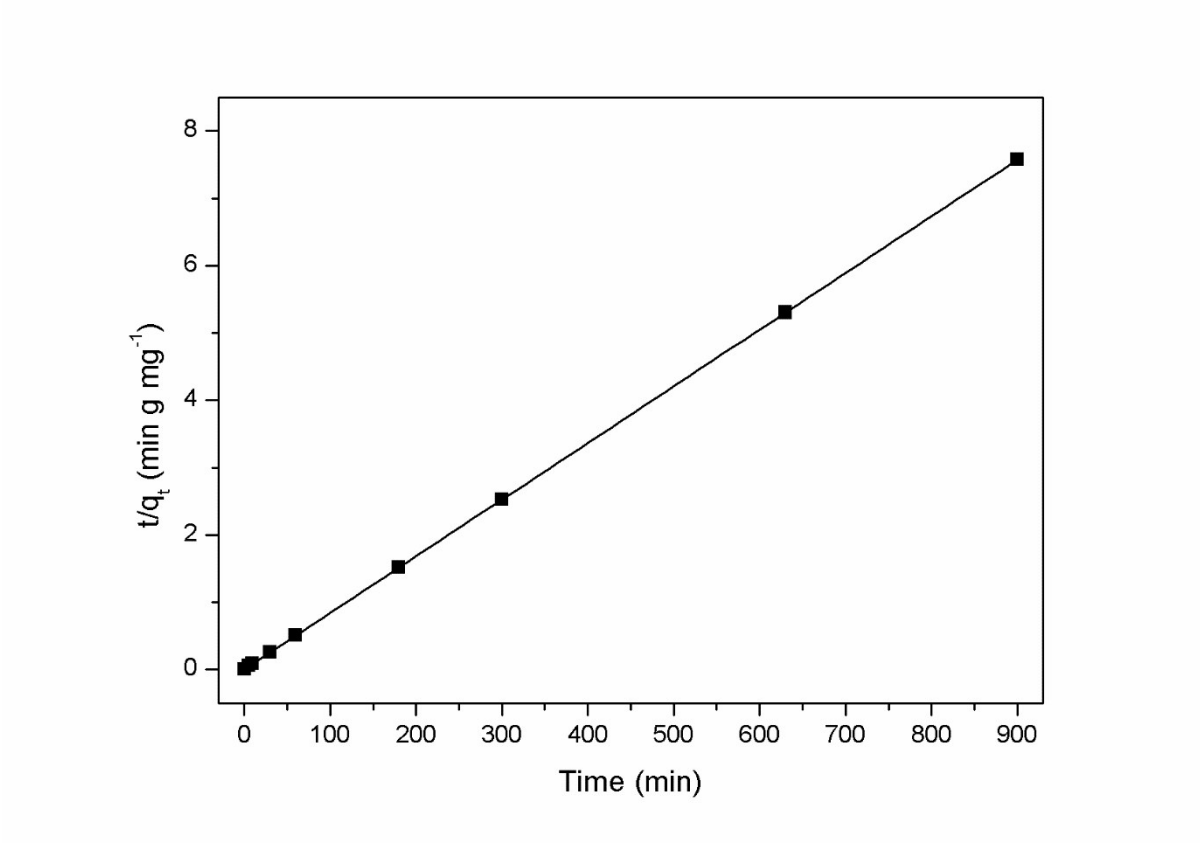

The kinetic investigation of PS_2DVS-SH under initial mercury ion concentration of 11.5 ppm were fitted with the pseudo-second-order kinetic model using equation S1, where k_2 (g mg^{-1} min^{-1}) is the rate constant of pseudo-second-order adsoprtion, t is time, and q_t and q_e are the amount of mercury adsorbed at time t and equilibrium.

$$\frac{t}{q^t} = \frac{t}{q^e} + \frac{1}{K_2 {q_e}^2} \quad \text{(S1)}$$

An extremely high correlation coefficient (>0.9999) was obtained between time (t) and t/Q_t. In addition, the adsorption rate constant of pseudo-second-order adsorption k_2 was determined to be 0.08 g mg^{-1} min^{-1}.

Figure S10. EDS images and spectra of PS_3DVS nanoparticles.

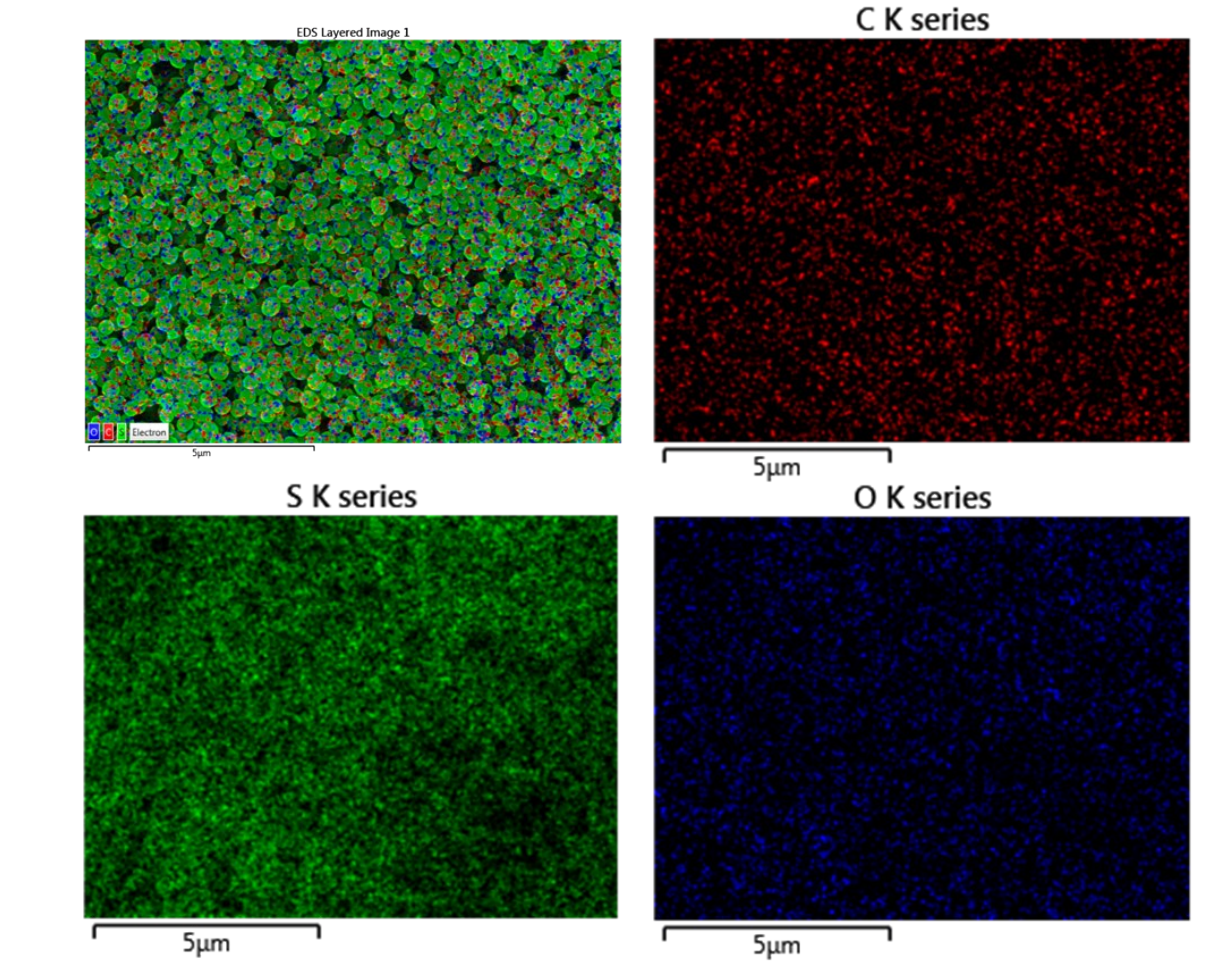

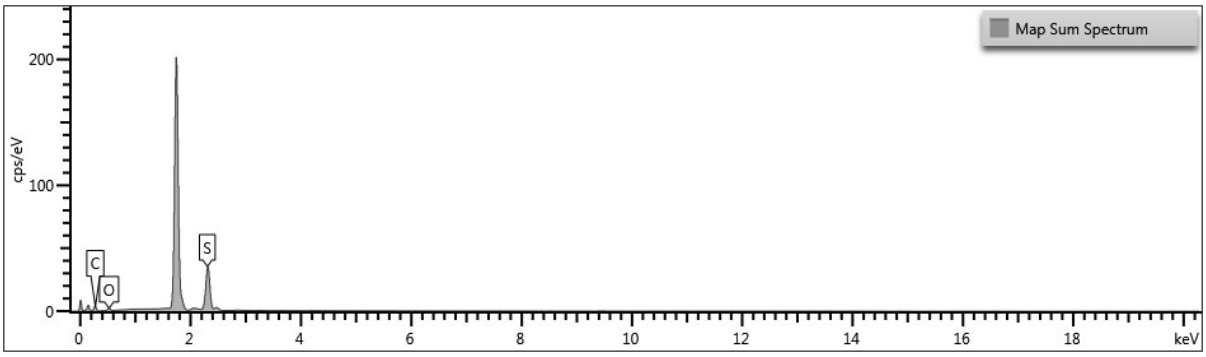

Figure S11. EDS images and spectra of mercury adsorbed PS_4DVS-SH nanoparticles before and after after iterative washing by DI water.

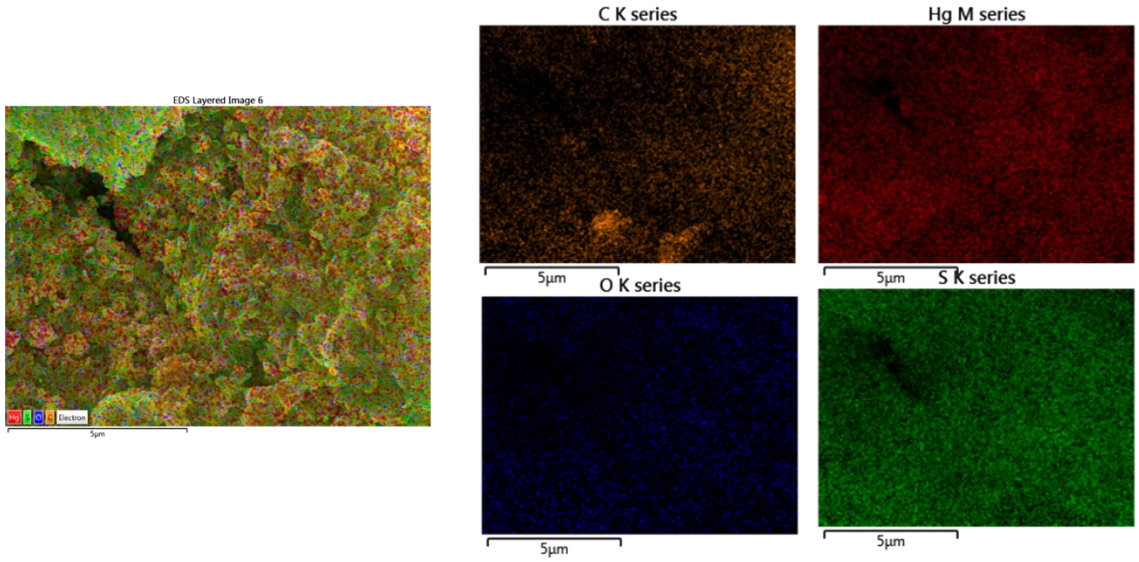

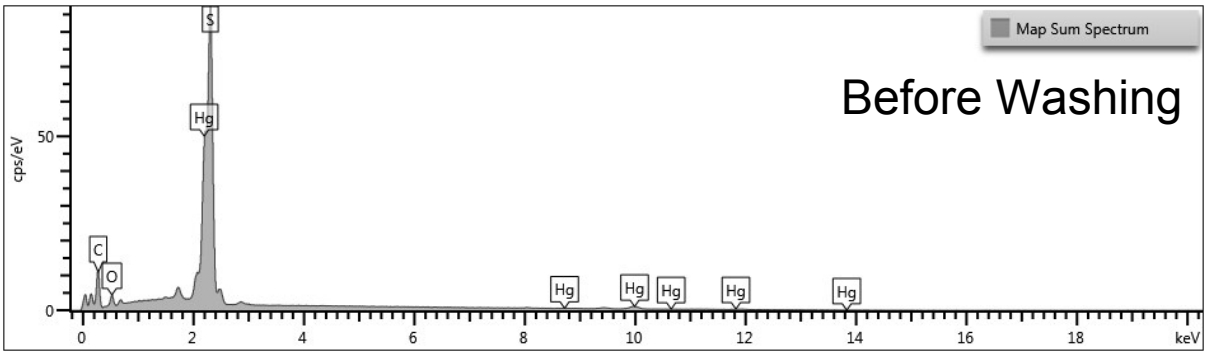

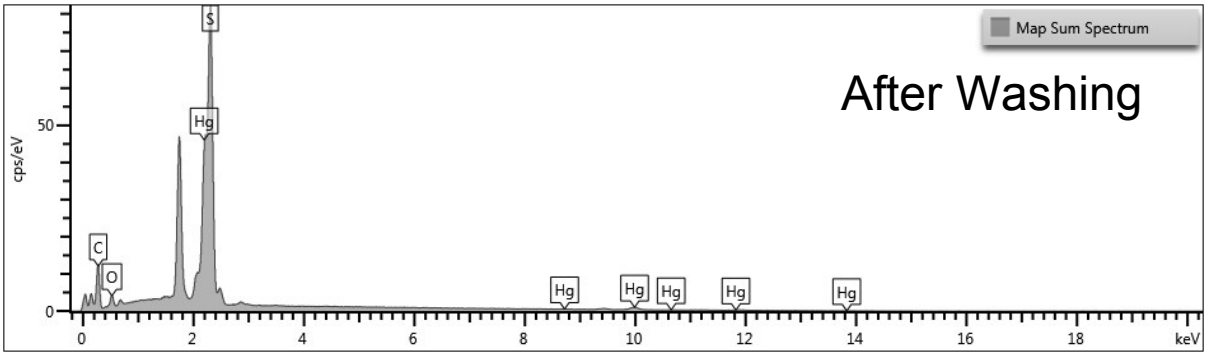

Figure S12. Hg 4f XPS spectra of mercury adsorbed PS_4DVS-SH.

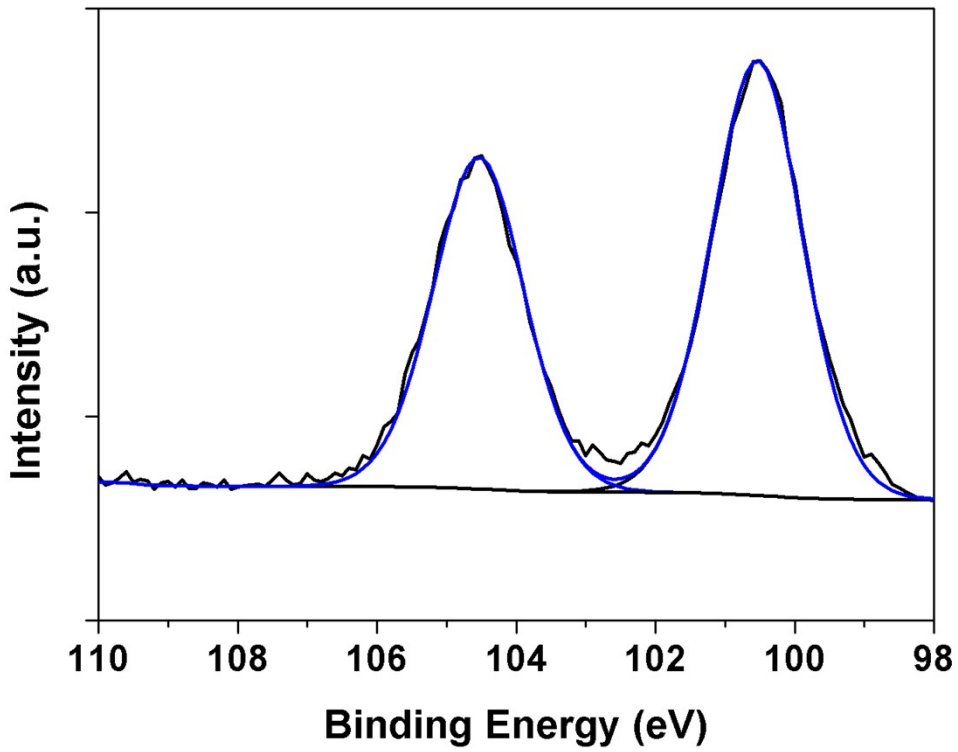

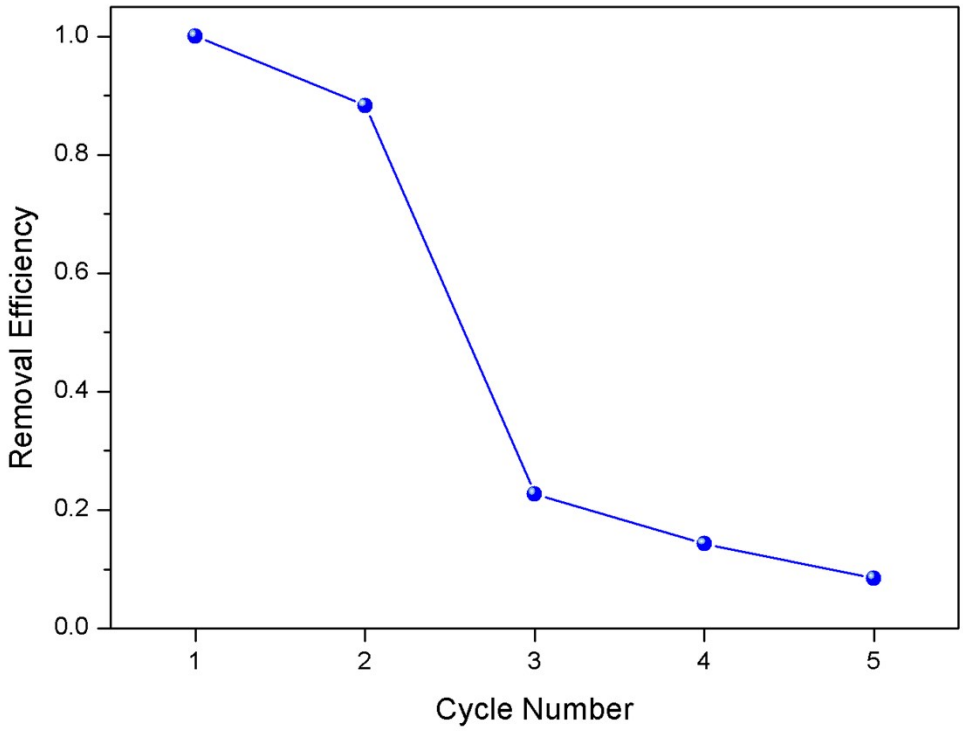

Figure S13. Reusability test of PS_4DVS-SH at 50 ppm Hg^{2+}.